

In vivo dendritic calcium dynamics in deep-layer cortical pyramidal neurons

Fritjof Helmchen¹, Karel Svoboda², Winfried Denk¹ and David W. Tank¹

¹ Biological Computation Research Department, Bell Laboratories, Lucent Technologies, Murray Hill, New Jersey 07974, USA

² Cold Spring Harbor Laboratory, Cold Spring Harbor, New York 11724, USA

Correspondence should be addressed to F.H. (fritjof@physics.bell-labs.com)

Dendritic Ca²⁺ action potentials in neocortical pyramidal neurons have been characterized in brain slices, but their presence and role in the intact neocortex remain unclear. Here we used two-photon microscopy to demonstrate Ca²⁺ electrogenesis in apical dendrites of deep-layer pyramidal neurons of rat barrel cortex *in vivo*. During whisker stimulation, complex spikes recorded intracellularly from distal dendrites and sharp waves in the electrocorticogram were accompanied by large dendritic [Ca²⁺] transients; these also occurred during bursts of action potentials recorded from somata of identified layer 5 neurons. The amplitude of the [Ca²⁺] transients was largest proximal to the main bifurcation, where sodium action potentials produced little Ca²⁺ influx. In some cases, synaptic stimulation evoked [Ca²⁺] transients without a concomitant action potential burst, suggesting variable coupling between dendrite and soma.

Voltage-dependent conductances in dendritic membranes enhance the computational power of dendrites in several ways. Under some conditions, sodium action potentials (Na⁺APs) backpropagate into the dendritic tree^{1,2} and might therefore regulate synaptic efficacy depending on dendritic Ca²⁺ accumulations during coincident pre- and postsynaptic activity^{3,4}. In addition, neocortical pyramidal cell dendrites are capable of producing regenerative electrical signals themselves^{5,6}, including Na⁺APs as well as calcium action potentials (Ca²⁺APs). Dendritic electrogenesis may be important to amplify distal synaptic currents, which otherwise would be relatively ineffective in depolarizing the soma^{5,7,8}. Dendritic Ca²⁺APs also have been implicated in the generation of bursts of Na⁺APs^{9–11}, in particular in ‘intrinsically bursting’ (IB) neurons in layer 5 of the neocortex^{12,13}. Bursts could provide a more reliable mode of information transfer than single APs¹⁴ and might be involved in cortical synchronization and oscillations¹⁵. Finally, calcium entering during dendritic electrogenesis acts as a biochemical messenger affecting various intradendritic signaling pathways.

Ca²⁺ electrogenesis in neocortical neurons is observed while pharmacologically reducing K⁺ currents^{16–19}. More evidence for Ca²⁺APs in dendrites of layer 5 pyramidal neurons is found in brain slice preparations using direct dendritic recordings^{5,6,11,20–22}, local glutamate iontophoresis²³ and calcium imaging^{5,19}. The question remains, however, how these results relate to the situation in the intact brain, as background synaptic activity²⁴, inhibitory inputs^{11,25,26} and neuromodulatory afferents²⁷ can affect the initiation of regenerative dendritic signals and their coupling to the soma. So far, only a few observations, including complex spiking behavior in direct dendritic recordings^{28,29} and slow depolarizing events that remained after the blockade of Na⁺ and K⁺ channels^{30–32}, provide evidence for dendritic Ca²⁺ electrogenesis in neocortical neurons *in vivo*.

In previous studies on layer 2/3 pyramidal neurons^{33,34}, in which *in-vivo* dendritic calcium dynamics were measured using two-photon laser scanning microscopy^{35,36} (2PLSM), Ca²⁺ influx into the

proximal dendrites strictly depended on the spread of Na⁺APs. Although dendritic current injection could evoke Ca²⁺APs in some layer 2/3 cells³⁴, no evidence was found for dendritic Ca²⁺ electrogenesis occurring spontaneously or during sensory stimulation. Here, we measured *in vivo* calcium dynamics in apical dendritic tufts of deep-layer pyramidal neurons using either dendritic or somatic intracellular recordings in combination with 2PLSM. In contrast to the findings in layer 2/3 neurons, we found evidence for dendritic Ca²⁺ electrogenesis during sensory stimulation and in conjunction with burst firing.

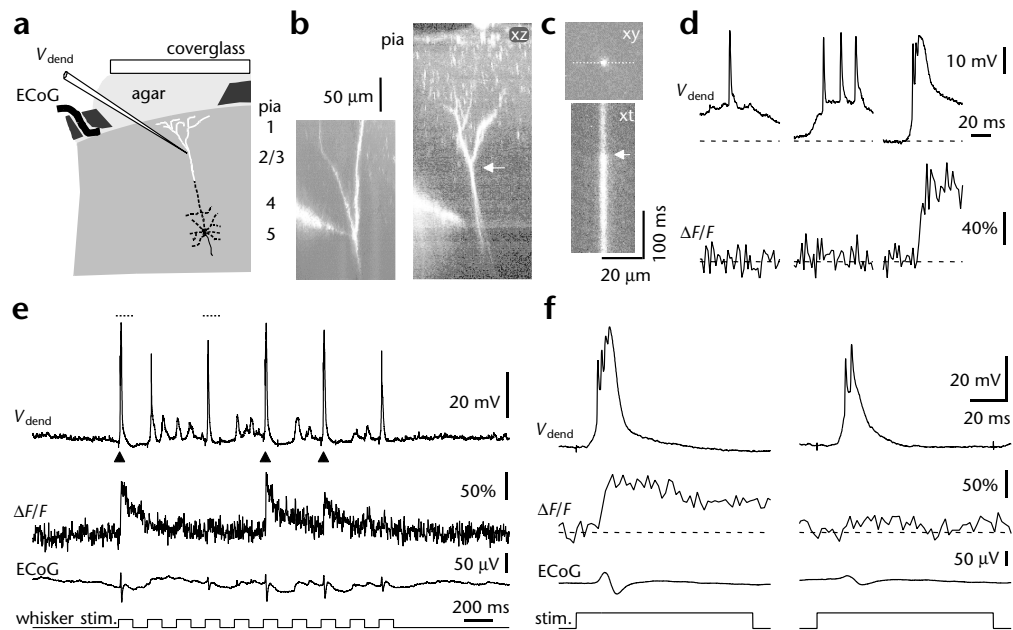
RESULTS

Sensory-evoked complex spikes and [Ca²⁺] transients

During previous studies on layer 2/3 pyramidal cells^{33,34}, we occasionally obtained recordings from dendrites of deeper neocortical neurons ($n = 6$; Fig. 1a). Dendritic impalement sites were 180 to 360 μm below the brain surface. Dendrites had a prominent bifurcation, but no soma was found down to about 500 μm , the maximum currently achievable imaging depth^{34,37} (Fig. 1b). In these recordings, Na⁺APs were rather small and broad, with an average amplitude of 30.0 ± 6.3 mV (mean \pm s.e.) from threshold and a half width of 1.39 ± 0.13 ms ($n = 6$; Fig. 1d). Dendritic Ca²⁺ influx was determined from the time course of Calcium Green-1 (CG-1) fluorescence at specific dendritic locations using the line-scan technique (Fig. 1c). Near the main bifurcation, single and even multiple Na⁺APs—either occurring spontaneously or evoked by whisker stimulation—did not cause detectable [Ca²⁺] transients (Fig. 1d). Closer to the soma, however, more than 100 μm proximal to the bifurcation, small Na⁺AP-evoked [Ca²⁺] transients were seen (3 of 3 cells; data not shown; $17.0 \pm 4.5\%$ $\Delta F/F$ per single Na⁺AP).

Sensory stimulation also could evoke ‘complex’ spikes, accompanied by large [Ca²⁺] transients, in the dendrites (Fig. 1d–f). Complex spikes arose from postsynaptic potentials (PSPs) evoked by whisker deflections, and were characterized by large, slow depolar-

Fig. 1. Dendritic recordings from deep neocortical pyramidal neurons. (a) Schematic of the recording configuration. Cells were filled with Calcium Green-1 via a dendritic impalement. The electrode and the distal dendrites, indicated in white, but not the soma could be imaged using 2PLSM. (b) Side-projections (*x-z* images) of two dendritic tufts obtained from stacks of 2PLSM fluorescence images. Recording electrodes are visible to the left of dendrites. The pial surface can be seen in the right example. The arrow indicates the position of the image and the line-scan data shown in (c) and (d). (c, top) Single fluorescence *x-y* image of the right stack in (b) at a focal plane about 10 μm below the main bifurcation. (c, bottom)



Line-scan image (*x* versus time; time running from top to bottom) for the dendritic cross-section in the *x-y* image as indicated by the dotted line. A complex spike caused a transient fluorescence increase (arrow). (d) Single or multiple Na^+ APs (V_{dend}) did not evoke detectable $[\text{Ca}^{2+}]$ transients ($\Delta F/F$) at this location (left and middle). A complex spike evoked by a whisker deflection, however, caused a large $[\text{Ca}^{2+}]$ transient (right). (e) Simultaneous recording of dendritic membrane potential, CG-1 fluorescence, and ECoG during a 2-s period of whisker stimulation (different cell from d). $[\text{Ca}^{2+}]$ transients only occurred in conjunction with complex spikes (arrowheads). Also note the whisker-evoked sharp spikes in the ECoG. (f) The responses to the first (left) and the fourth (right) whisker deflection expanded in time (dotted lines in e). The first whisker deflection evoked a complex spike and a $[\text{Ca}^{2+}]$ transient with a risetime corresponding to the width of the slow depolarization. The fourth deflection evoked two Na^+ APs, but no large, slow depolarization and no $[\text{Ca}^{2+}]$ transient. Fluorescence traces in (e) and (f) were measured $<50 \mu\text{m}$ proximal to the main bifurcation.

izations with superimposed bursts of two to five Na^+ APs. The depolarizations had amplitudes between 10 and 46 mV (from Na^+ AP threshold) and half widths between 10 and 35 ms. The CG-1 fluorescence transients associated with complex spikes had an average amplitude of $103 \pm 15\%$ and a decay time constant of 205 ± 39 ms near the bifurcation ($n = 6$). Several lines of evidence indicate that the observed Ca^{2+} influx occurred through voltage-dependent Ca^{2+} channels in the dendrite. First, large dendritic $[\text{Ca}^{2+}]$ transients could be elicited by dendritic current injections ($n = 3$; data not shown). Second, the rise of the $[\text{Ca}^{2+}]$ transients correlated well with the duration of the slow depolarization (Fig. 1f); in fact, the integral of the voltage trace superimposed well on the rising phase of the fluorescence signal (Fig. 2a). Third, the amplitudes of slow depolarizations and $[\text{Ca}^{2+}]$ transients varied in a graded manner and were highly correlated in three experiments (Fig. 2b and c).

Whisker deflections caused spike-like sharp waves in the electrocorticogram (ECoG) recordings (Fig. 1d and e). The time courses of these events resembled the derivative of the smoothed intracellular voltage traces (Fig. 2a), and the amplitudes of the ECoG spikes and the slow depolarizations were correlated ($r = 0.51-0.92$; $n = 3$; Fig. 2d). Postsynaptic currents and dendritic Ca^{2+} influx during complex spikes, occurring synchronously in a large population of neurons³⁸, most probably sum and contribute to the upper-neocortical-layer current sink that causes the spike in the ECoG³⁹.

$[\text{Ca}^{2+}]$ transients during burst firing in layer 5 cells

Based on the similarities of the observed complex spikes to published dendritic recordings²⁹, we strongly suspected that our record-

ings were from apical dendrites of layer 5 pyramidal neurons. To confirm this, we measured dendritic calcium dynamics in identified layer 5 neurons, using impalements made 800 to 1200 μm below the pia, near the location of somata of layer 5 neurons (Fig. 3a). Several technical problems had to be overcome. First, electrode tips were too deep to be imaged and, therefore, could not serve as direct guide to the cells; dendritic tufts often could, however, be found by triangulation, based on the depth and angle of the electrode (see Methods). Second, diffusional dye loading of the dendritic tree via the soma was rather slow and dendrites could not be found for at least 45 minutes. Third, impaled neurons could lack dendrites in the superficial layers. To increase the likelihood of finding dendrites, we focused on intrinsically bursting (IB) neurons, which are layer 5 pyramidal cells with extensive apical tufts reaching up to layer one^{12,13,21,40}.

Using this approach, the apical tufts of 12 layer 5 IB neurons were found with two-photon microscopy (Fig. 3b). In five of these cases, the tuft was found with the electrical recording still maintained, so that somatic membrane potential and dendritic fluorescence changes could be measured simultaneously. In four of the remaining seven experiments, large $[\text{Ca}^{2+}]$ transients were evoked by synaptic stimulation. In three cases, no clear $[\text{Ca}^{2+}]$ transients were detected, possibly because only distal tuft branches were found, with the main bifurcation either too deep to be imaged or obstructed by surface blood vessels. Eight neurons were recovered histologically following neurobiotin injections, confirming that voltage recordings and imaging were from layer 5 pyramidal cells (Fig. 3b). The average resting potential and input resistance were -73 ± 2 mV and 31 ± 3 M Ω , respectively ($n = 12$). Na^+ APs had

larger amplitudes and shorter durations than those in the dendritic recordings, with an average amplitude of 60 ± 3 mV from threshold and a half width of 0.69 ± 0.03 milliseconds. Individual Na^+ APs often were followed by a prominent depolarizing after-potential (Fig. 3c). Although small fluorescence transients (about 10% change) evoked by single- Na^+ APs were seen in 2 cells 150–300 μm below the main bifurcation (at the maximum imaging depth, ~ 500 μm), individual or repetitive Na^+ APs did not cause detectable $[\text{Ca}^{2+}]$ transients near the main bifurcation ($n = 5$; Fig. 3c).

In contrast, burst firing in layer 5 neurons usually was associated with large dendritic $[\text{Ca}^{2+}]$ transients (Fig. 3c and d). Bursts typically consisted of 3–5 Na^+ APs (200–400 Hz intraburst frequency) of decreasing amplitude, superimposed on a slow depolarizing potential. Bursts occurred spontaneously (0.15–3 per second), but could also be evoked by somatic current injection or sensory stimulation. Current injection-evoked bursts were always accompanied by dendritic $[\text{Ca}^{2+}]$ transients, suggesting that voltage-dependent Ca^{2+} channels rather than ligand-gated synaptic receptors were the source of calcium influx during bursts. The average amplitude of fluorescence transients associated with bursts was $85 \pm 15\%$ proximal to the bifurcation, and the average decay time constant was 200 ± 22 milliseconds ($n = 9$); these values are similar to those for the $[\text{Ca}^{2+}]$ transients observed with dendritic impalements. As in the dendritic recordings, the rise in fluorescence traced the slow, depolarizing potential underlying the bursts (Fig. 3c and d). The slow-potential envelope had an amplitude of about 20 mV and, unlike that for the dendritic recordings, a plot of peak fluorescence changes versus envelope amplitude revealed discrete clustering of the data points into two groups, suggesting an all-or-none phenomenon ($n = 3$ cells; Fig. 3e). Taken together, these findings suggest that Ca^{2+} APs were generated in the apical dendrite and could be coupled to bursts of APs. The slow potential may represent the attenuated remains of the dendritic Ca^{2+} AP at the soma; therefore, the dendritic Ca^{2+} AP may be responsible for triggering the Na^+ APs later in the burst¹¹. Although a co-occurrence of $[\text{Ca}^{2+}]$ transients in the apical dendrite and bursts of APs was observed in most cases, we also found cases in which either large $[\text{Ca}^{2+}]$ transients or bursts of APs occurred alone (see below).

Variable coupling of $[\text{Ca}^{2+}]$ transients and bursts

The relationship between bursts and dendritic $[\text{Ca}^{2+}]$ transients was further investigated using sensory stimulation or synaptic activation via a surface electrode. Whisker deflections evoked variable cellular responses (Fig. 4). The cell shown in Figure 4a, for example, had a relatively high level of background activity with spontaneously occurring bursts and accompanying $[\text{Ca}^{2+}]$ transients. Repetitive whisker stimulation evoked additional bursts associated with $[\text{Ca}^{2+}]$ transients. The first in the series of whisker deflections, however,

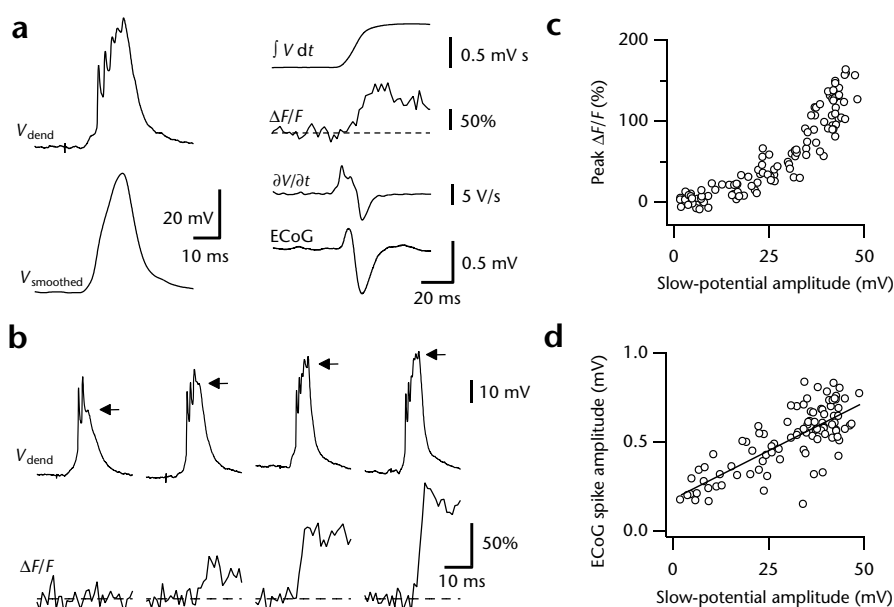


Fig. 2. Relationship between dendritic complex spikes, $[\text{Ca}^{2+}]$ transients and ECoG spikes. **(a)** (left) Filtering of a sensory-evoked complex spike results in a smooth curve approximating the time course of the underlying depolarization. The integral of the smoothed voltage trace resembles the rise of the fluorescence trace (right, upper traces) indicating calcium influx during the slow depolarization. The derivative of the smoothed voltage trace resembles the sharp spike observed in the ECoG trace (right, lower traces). **(b)** Variability of the amplitudes of the slow depolarization (arrows) and the $[\text{Ca}^{2+}]$ transient. Larger depolarizations evoked larger fluorescence changes. **(c)** Peak fluorescence changes plotted versus the amplitude of the slow depolarizations (measured from Na^+ AP threshold). **(d)** Correlation between the amplitudes of ECoG spikes (measured between minimum and maximum) and those of slow depolarizations. The linear regression coefficient in this example was $r = 0.82$. All data were obtained from line-scans measured < 50 μm proximal to the main bifurcation of the same cell as in Fig. 1e and f.

evoked a large dendritic $[\text{Ca}^{2+}]$ transient but only a single Na^+ AP ($n = 14$ trials; Fig. 4a). The rising phase of this $[\text{Ca}^{2+}]$ transient coincided with the PSP and the ECoG spike (left traces in Fig. 4b). The observation of a clear $[\text{Ca}^{2+}]$ transient in the absence of associated multiple Na^+ APs indicates that a dendritic Ca^{2+} AP does not inevitably lead to a burst of Na^+ APs. One possible explanation for this decoupling of $[\text{Ca}^{2+}]$ transients and bursts is that simultaneously activated inhibitory inputs shunt the current flow from the dendrite to the soma, thereby preventing the generation of a burst. Consistent with this idea, the amplitude of single Na^+ APs evoked by initial whisker deflections was reduced by 9.2 ± 0.5 mV ($n = 14$ trials) compared with the pre-stimulus amplitude of spontaneous Na^+ APs in this cell (Fig. 4a); in 8 other cells a 4–12 mV reduction was observed. Although some Na^+ APs preceding bursts during subsequent deflections were reduced in size as well (range, 0–7 mV; mean 2.4 ± 0.3 mV; $n = 30$ bursts in the cell in Fig. 4a), this reduction was not as strong as with the first deflection. Another type of response was observed in four cells in which the first whisker deflection, in most cases, caused an immediate burst of APs (Fig. 4c). Although we do not have simultaneous fluorescence and voltage recordings for this immediate burst response, a dendritic $[\text{Ca}^{2+}]$ transient was seen in response to an initial deflection in one of these cells after the electrical recording had been lost (Fig. 4c); this suggests that, in these cases, initial whisker deflections caused large dendritic depolarizations, triggering Ca^{2+} influx and a burst of APs similar to the sensory-evoked complex spikes in our dendritic recordings. A third type of response was seen in four IB neurons following whisker deflections that were not the first in a series of stimuli. In these cases, bursts of APs occurred with a variable delay

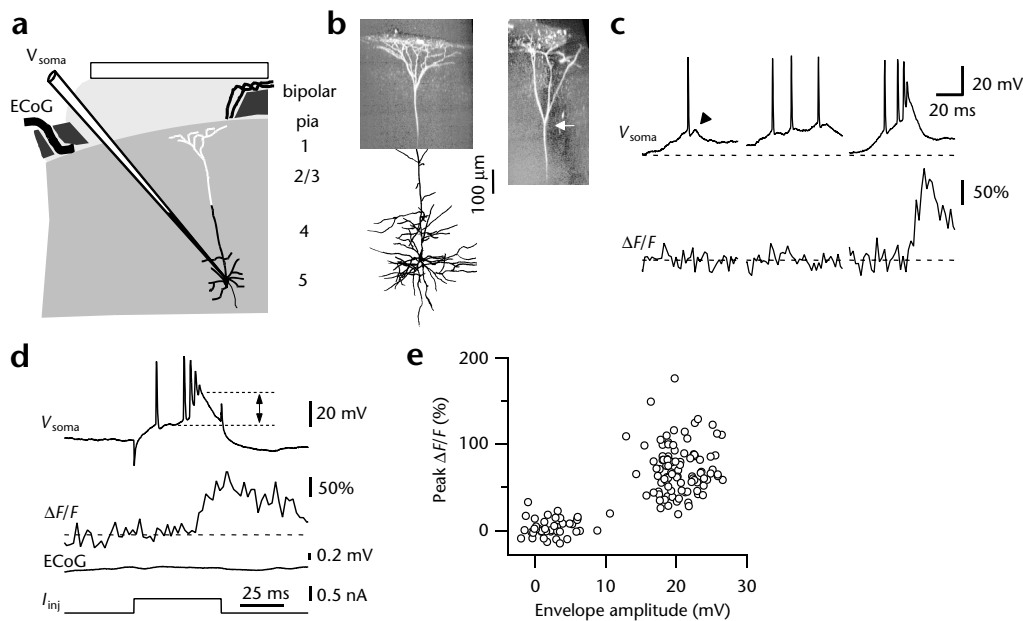


Fig. 3. Simultaneous somatic recording and distal dendritic imaging from intrinsically bursting layer 5 neurons. **(a)** Experimental configuration for somatic recordings. The distal apical tuft (white) could be imaged using 2PLSM. The lower part of the electrode and the proximal part of the neuron (black) were not visible. In addition to whisker stimulation, a bipolar electrode sometimes was used for synaptic stimulation. **(b)** Side projections of two apical tufts. The left layer 5 neuron was recovered histologically, and a collage of the neurobiotin reconstruction (lower part) and the fluorescence image (upper part) is shown. The

arrow indicates the location for the line-scans shown in **(c)**. **(c)** Single or multiple Na⁺APs (V_{soma}) did not evoke detectable [Ca²⁺] transients ($\Delta F/F$) near the main bifurcation of the right cell in **(b)** (left and middle). At the same location a spontaneous burst of Na⁺APs superimposed on a slow depolarizing potential caused a large [Ca²⁺] transient (right). Note the depolarizing afterpotential following the single Na⁺AP (arrowhead). **(d)** Somatic current injection (50 ms) evoked a burst of action potentials and a large simultaneous [Ca²⁺] transient 70 μm proximal to the main bifurcation of a different cell. The rise in fluorescence correlates with the slow depolarization underlying the burst. **(e)** Peak fluorescence changes plotted versus the envelope amplitude of the slow depolarization (as indicated in **d**). The right cluster of data points corresponds to bursts (either spontaneous ones or evoked by whisker stimulation or current injections) and the associated [Ca²⁺] transients, whereas the left cluster represents control traces in which only a single Na⁺AP but no burst was elicited. The clustering into two groups suggests that bursts occurred in an all-or-none manner.

with respect to the PSP onset (mean latency about 20 ms). In the example shown in Fig. 4a, these bursts were associated with dendritic [Ca²⁺] rises which were delayed as well and coincided with the slow potential underlying the bursts (Fig. 4b).

To activate a different pattern of synaptic input, most likely via distal afferents in layer 1, we also used brain surface stimulation (see Fig. 3a). Suprathreshold EPSPs were evoked in seven cells, causing either a single Na⁺AP or a brief burst of APs. In one experiment, simultaneous recording of voltage and fluorescence again revealed a large dendritic [Ca²⁺] transient associated with only a single Na⁺AP (Fig. 5a; three trials), similar to the response to some initial whisker deflections (Fig. 4a). Supporting the idea that a dendritic Ca²⁺AP occurred but that burst generation was suppressed by coactivated inhibitory inputs, the Na⁺AP amplitude was reduced by 10 ± 1 mV ($n = 3$ traces) compared with spontaneous APs, and subthreshold EPSPs were followed by a hyperpolarization, presumably due to inhibitory PSPs (Fig. 5b).

In summary, there seemed to be at least two types of dendritic [Ca²⁺] transients in IB neurons. In the first, immediate transients occurred simultaneously with the PSP and were accompanied by either a burst or a single Na⁺AP. Presumably, synaptic activation in these cases caused large depolarizations in the apical dendrite, possibly involving amplification of synaptic currents via dendritic Ca²⁺ electrogenesis. Whether a single Na⁺AP or a burst was generated then depended on the location and strength of simultaneously activated inhibitory inputs. In the second, delayed transients followed the PSP with a latency of at least ten milliseconds and were associated with intrinsic bursts of APs. In this case, the net dendritic excitation was presumably not large

enough to initiate dendritic Ca²⁺ influx immediately, but still sufficient to trigger a delayed dendritic Ca²⁺AP.

A different type of decoupling of dendritic [Ca²⁺] transients and bursts of APs was observed in some cases of spontaneous bursts. Although spontaneous bursts were associated with dendritic [Ca²⁺] transients in most cases (95 transients in 3 cells), they occasionally were observed without a concomitant [Ca²⁺] transient ($n = 10$ in 2 cells; Fig. 5c). These bursts might have been triggered by a Ca²⁺AP in a different dendritic branch, for instance, in the basal dendrites.

Spatial profile of dendritic [Ca²⁺] transients

The [Ca²⁺] transient amplitude was mapped as a function of depth below the pia to estimate in which part of the dendritic tree most of the calcium influx during bursts occurred, and, therefore, where dendritic Ca²⁺APs were most likely to be initiated (Fig. 6). In apical tufts filled via both somatic (four of four IB neurons tested) and dendritic impalements (two of two tufts), [Ca²⁺] transients were largest proximal to the main bifurcation, and decreased in amplitude along the secondary and tertiary branches of the tuft (Fig. 6c and d). The steepest fall-off in the [Ca²⁺] transient profile consistently occurred distal to either the main bifurcation or the secondary bifurcations (Fig. 6e). Although not every distal tuft branch was examined, these findings suggested that the dendritic Ca²⁺APs during bursts were generated in the apical trunk rather than in the apical tuft branches.

DISCUSSION

In this paper we describe *in vivo* measurements of dendritic calcium dynamics in deep-layer pyramidal neurons. Compared with

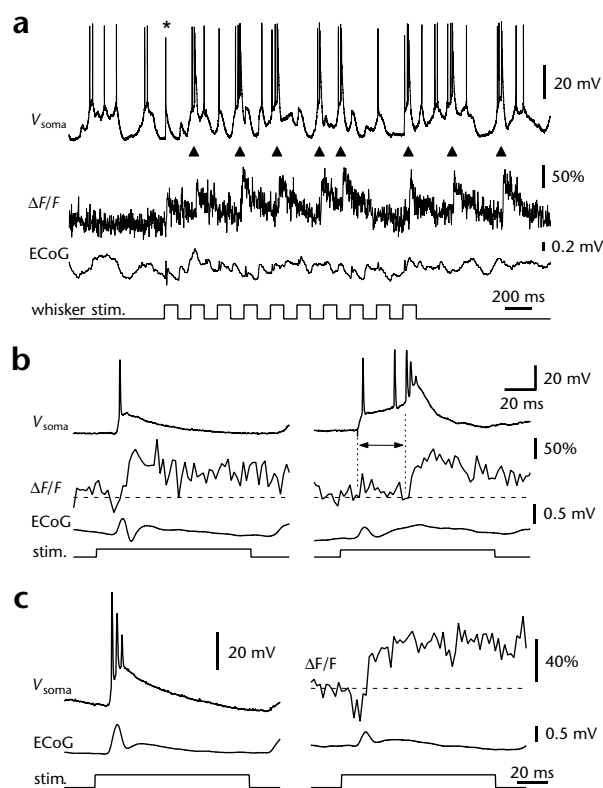


Fig. 4. Sensory-evoked dendritic $[Ca^{2+}]$ transients in layer 5 neurons. (a) Simultaneous recording of somatic membrane potential (V_{soma}), CG-1 fluorescence about 50 μm proximal to the main bifurcation ($\Delta F/F$) and ECoG during a 2-s period of whisker stimulation. Large $[Ca^{2+}]$ transients occurred in conjunction with bursts (arrowheads), both spontaneously and during whisker deflections. The first whisker deflection evoked a dendritic $[Ca^{2+}]$ transient, but only a single Na^+ AP of reduced amplitude (marked by an asterisk). As in Fig. 1d, spikes in the ECoG were observed. (b) The response to the first and the last whisker deflection in (a), expanded in time. The first whisker deflection failed to evoke a burst in this case, but caused a large transient which coincided with the PSP and the ECoG spike (left). The last whisker deflection evoked a burst and an associated $[Ca^{2+}]$ transient with a delay after the PSP (arrow). The fluorescence rise in this case traced the slow depolarization underlying the burst. (c) A different neuron responded to a first whisker deflection of a series with a burst of Na^+ APs riding on the PSP (left). After the apical tuft had been found for imaging but the electrical recording had been lost, a $[Ca^{2+}]$ transient near the main bifurcation was evoked with no delay by an equivalent stimulus (right).

previous findings on superficial pyramidal neurons^{33,34}, our findings present a very different picture. Most notably, we showed dendritic Ca^{2+} electrogenesis in deep neocortical neurons in the intact brain upon sensory stimulation and during intrinsic bursting. The apical dendrite seemed to act as an integrative compartment separate from the soma, and evidence was found for variable coupling between dendrite and soma.

Somatic versus dendritic recordings

Neocortical pyramidal neurons can be classified based on their firing properties as either regularly spiking (RS) or intrinsically bursting (IB)¹², although several subclasses may exist^{41,42}. IB neurons were first described in brain slices^{13,16,40}, and have also been found *in vivo*^{29,30,42}. Whereas the somatic recordings reported here were unambiguously from layer 5 IB neurons, the identity of the neurons in the dendritic recordings was less certain, since they were not recovered histologically. For several reasons, we think that some, if not all, of these dendrites belonged to layer 5, but not nec-

essarily IB, pyramidal neurons. First, like identified layer 5 tufts^{13,40}, all tufts had a thick apical dendrite with a prominent bifurcation, but few or no oblique branches. Second, the complex pattern of Na^+ APs riding on a broad depolarization (Fig. 1 and 2) is similar to what is seen in dendritic recordings from identified layer 5 neurons *in vitro*^{6,11,20}. Third, recent dendritic patch recordings *in vivo* showed similar complex spikes which were attributed to layer 5 neurons²⁹. Also, the small amplitude and large half-width of the Na^+ APs in our dendritic recordings were consistent with impalement sites more than 500 μm from the soma, based on recordings from distal dendrites of layer 5 neurons in brain slices⁶. We cannot fully exclude the possibility, however, that our dendritic recordings were from deep layer 3 or layer 4 pyramidal neurons with somata 500–800 μm below the pia. In any case, the dendritically recorded neurons closely resembled the identified layer 5 neurons with respect to dendritic calcium dynamics, but differed from superficial pyramidal neurons. No spontaneous complex spikes were observed in the dendritic recordings. It is possible that some of these recordings were from RS neurons, because some RS neu-

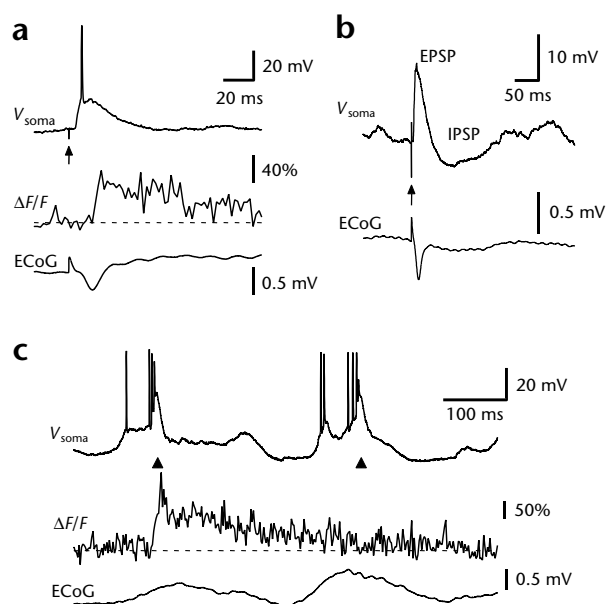


Fig. 5. $[Ca^{2+}]$ transients in the apical dendrite and somatic bursts of APs can occur in isolation. (a) Example of a suprathreshold response to brain surface stimulation (arrow). A large $[Ca^{2+}]$ transient near the main bifurcation of an IB neuron but only a single Na^+ AP were elicited, resembling the response to the first whisker deflection in Fig. 4b. Note that surface stimulation also caused an ECoG spike. (b) Subthreshold response to surface stimulation in the same neuron shown on a slower time scale (average of five traces). The initial EPSP was followed by a putative IPSP, suggesting that shunting inhibition suppressed the generation of a burst in (a). (c) Example of a spontaneous Na^+ AP burst without a concomitant dendritic $[Ca^{2+}]$ transient (right arrowhead). A spontaneous burst of similar shape 250 ms earlier did cause a large $[Ca^{2+}]$ transient (left arrowhead).

rons possess extensive apical tufts^{40,41}, and because RS like IB neurons can respond to synaptic stimulation with bursts¹¹.

Comparison to layer 2/3 pyramidal neurons

In layer 2/3 pyramidal cell dendrites in the intact cortex, calcium influx depends strictly on Na⁺APs that rapidly decrease in amplitude with distance from the soma and fail to actively invade the distal dendrites^{33,34}. In contrast, in our dendritic recordings of presumed layer 5 neurons, Na⁺APs had a reduced but still considerable amplitude near the main bifurcation, presumably several hundred micrometers from the soma; this suggests that Na⁺APs in layer 5 cells, unlike in layer 2/3 cells, backpropagate relatively far into the apical dendrite, although in a decremental fashion as in brain slices⁶ and awake rats⁴³. Single Na⁺APs evoked small [Ca²⁺] transients at the deepest dendritic sites investigated (~500 μm from the pia), but Na⁺AP-evoked [Ca²⁺] transients were not detectable near the main bifurcation. Either the Na⁺AP amplitude there was too small, or the voltage threshold or the kinetics of the dendritic Ca²⁺ channels at this location was such that they were not opened significantly by low-frequency Na⁺APs.

The most striking difference compared with layer 2/3 neurons, however, was the capability of layer 5 neurons to produce large [Ca²⁺] transients at distal dendritic locations where Na⁺APs did not cause detectable calcium influx. Whereas dendritic current injection can sometimes elicit Ca²⁺APs in layer 2/3 neurons³⁴, they have not been observed to occur spontaneously, nor could they be triggered by whisker stimulation. In contrast, in distal dendrites of layer 5 neurons, large [Ca²⁺] transients were seen under a variety of conditions, in particular, during sensory stimulation. The major component of the calcium influx presumably occurred through dendritic voltage-dependent Ca²⁺ channels, rather than through ligand-gated channels, as large [Ca²⁺] transients also occurred spontaneously and could be evoked by current injection. Most, but not all, [Ca²⁺] transients were associated with bursts of Na⁺APs, indicating the generation of dendritic Ca²⁺APs¹¹. Occasionally, spontaneous bursts occurred without a detectable dendritic [Ca²⁺] transient. Such bursts might have been initiated by

slow regenerative events in basal dendrites. More importantly, the response to synaptic stimulation was highly variable, ranging from immediate bursts to delayed bursts, and even to seemingly suppressed bursts. In the last case, large dendritic Ca²⁺ transients were accompanied by only a single Na⁺AP, suggesting that a large dendritic depolarization occurred in relative isolation from the soma⁵. A possible explanation for the variable responses to whisker deflections is that the generation and the timing of bursts were affected by simultaneous inhibitory inputs. In support of this interpretation, the amplitudes of some Na⁺APs were reduced during synaptic stimulation (see also ref. 26), and EPSPs evoked by surface stimulation were followed by a hyperpolarization. In brain slices, furthermore, inhibitory inputs onto the apical trunk effectively delay or suppress bursts and dendritic Ca²⁺APs^{11,25}.

Dendritic [Ca²⁺] transients were always largest proximal to the main bifurcation. Because of the inaccessibility of the entire proximal dendrite to imaging, we could not determine if an 'apical band' of Ca²⁺ accumulation as observed *in vitro* existed¹⁹. One explanation for the lack of [Ca²⁺] transients in the most distal branches could be a decrease in Ca²⁺-channel density. Alternatively, Ca²⁺APs, if generated in the apical trunk, could be attenuated while spreading into the tuft. Consistent with attenuation at dendritic branch points is that the spatial profiles of [Ca²⁺]-transient amplitude always showed the steepest fall-off distal to major dendritic bifurcations (Fig. 6). In contrast to our results, [Ca²⁺] transients in brain slices evoked by distal synaptic stimulation are largest in the tuft branches⁵. This could be because of differences in the stimulation pattern used, since we did not determine spatial profiles using brain-surface stimulation. Alternatively, Ca²⁺APs in distal dendritic branches may be attenuated more strongly *in vivo* compared to those in brain slices because of a lower input impedance resulting from synaptic background activity. In summary, our data

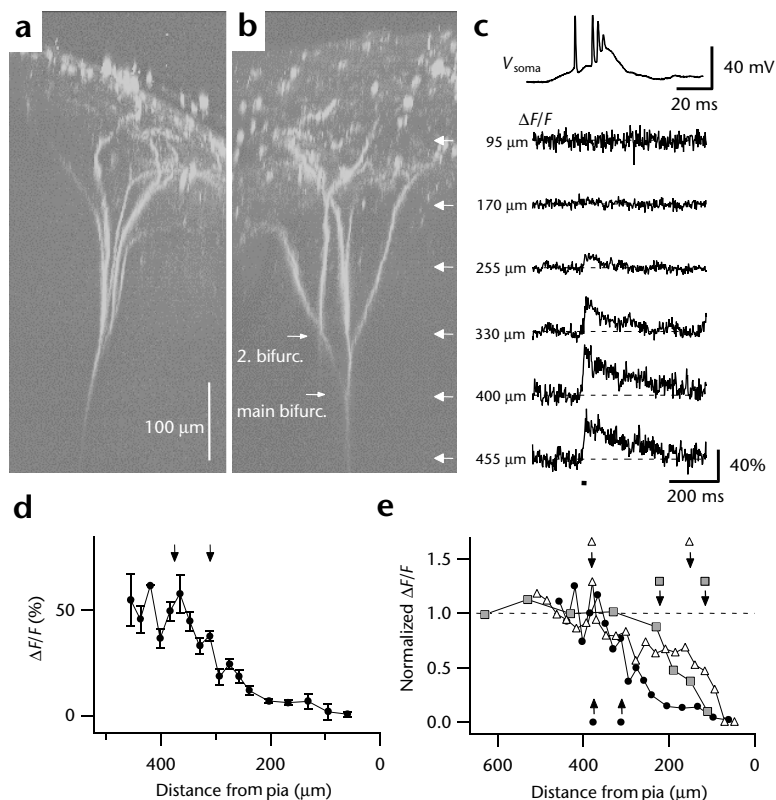


Fig. 6. Spatial profile of distal dendritic [Ca²⁺] transients. (a, b) Sagittal and coronal side-projections of an apical tuft of a layer 5 pyramidal neuron. The pial surface is slightly tilted. Note the main bifurcation and the secondary bifurcations at depths of about 370 μm and 310 μm, respectively. Arrows indicate the depth for the fluorescence recordings shown in (c). (c) Dendritic [Ca²⁺] transients (ΔF/F) associated with typical Na⁺AP bursts (V_{soma} , upper trace) were measured at different depth below the pia as noted. Bursts occurred spontaneously or during whisker stimulation at the time indicated by the short horizontal bar. Fluorescence traces are averages of 4 to 6 measurements. (d) Average amplitude of the [Ca²⁺] transients shown in (c) as a function of depth below the pial surface. The positions of the main bifurcation and the secondary bifurcations are indicated. (e) [Ca²⁺] transient profile for three different dendritic tufts with major bifurcations at different depths (tufts shown in a and b and in Fig 3b). [Ca²⁺] transient amplitudes were normalized to the mean value proximal to the main bifurcation. Arrows indicate the depth below the pia of the main bifurcation (left arrow) and the secondary bifurcations (right arrow). Note that in all cases, the steepest fall-off in the profile occurred distal to a major bifurcation. Solid circles are the same data as shown in (d).

are more consistent with a Ca^{2+} AP initiation site in the apical trunk, as found in prefrontal layer 5 neurons²².

Dendritic calcium spikes and burst generation

One possible mechanism for burst generation is the interaction between different, partially coupled electrogenic cell compartments^{10,44,45}. Our results are consistent with the idea that in IB neurons, backpropagating Na^+ APs can initiate a Ca^{2+} AP in the dendrite, which then, in turn, can lead to sustained current flow back into the soma, triggering additional Na^+ APs^{9,11}. However, a supplemental or essential role of persistent Na^+ currents to burst generation^{23,46} cannot be excluded. In addition, the observation of spontaneous bursts in the absence of $[\text{Ca}^{2+}]$ transients in the apical dendrite suggests that active currents in basal dendrites might be capable of generating bursts. Potentially, these currents might also have contributed to burst generation in those cases in which $[\text{Ca}^{2+}]$ transients were observed in the apical dendrite. Because Ca^{2+} -activated K^+ channels as well as Ca^{2+} -dependent Ca^{2+} -channel inactivation could be involved in burst termination⁴⁷, one might be concerned that bursting was induced by Ca^{2+} buffering⁴⁷. This possibility can however almost certainly be ruled out by the observation that bursts were seen immediately after the penetration. In addition, the indicator concentration in our experiments (about 100 μM , see Methods) was much lower than needed for burst induction ($> 5 \text{ mM}$)⁴⁷.

Our results thus confirm the idea that the apical dendrite of a layer 5 neuron constitutes an integrative compartment separate from the soma^{5,11,19}. A Ca^{2+} AP-trigger zone near the main bifurcation is well suited to integrate layer 1 inputs in a non-linear way, and then to send the result via current flow to the soma. Efficiency to depolarize the soma, however, is susceptible to inhibitory inputs²⁵ as well as neuromodulatory influences on the membrane conductances^{27,48}. Burst generation thus depends on the precise interaction between the two integrative compartments, and, therefore, may serve as an indicator of the associative activation of proximal and distal synaptic inputs¹¹. Another important functional aspect might be a differential effect of bursts on postsynaptic neurons, depending on whether these show depression or facilitation in response to repetitive synaptic stimulation⁴⁹. Further experiments using combined somatic recording and dendritic calcium imaging may elucidate the control of the coupling between dendrite and soma and the role of burst firing *in vivo*. In the future, it might be possible to investigate Ca^{2+} electrogenesis in distal apical dendritic tufts during different behavioral states in awake rodents using a head-mounted miniaturized two-photon microscope currently under development (F.H., M.S. Fee, D.W.T., W.D., *Soc. Neurosci. Abstr.* 25, 322.1, 1999).

METHODS

Preparation and electrophysiology. All experimental procedures were approved by the Bell Laboratories Institutional Animal Care and Use Committee. Sprague Dawley rats (100–400 g, 15 male, 3 female) were anesthetized with urethane (i.p., 1.5 g per kg body weight, $n = 17$) or with a mixture of ketamine and xylazine (i.m., $n = 1$ dendritic recording). A stainless steel frame was glued to the skull with dental cement at an angle of about 25° to the horizontal plane. A 3 × 3 mm craniotomy was cut above the somatosensory area corresponding to the barrel field and the dura was carefully removed. Motion induced by the animals breathing and heart beat was reduced by filling the craniotomy with 2% agarose (Type III-A, Sigma) in a solution containing 125 mM NaCl, 5 mM KCl, 10 mM glucose, 10 mM HEPES, 2 mM CaCl_2 and 2 mM MgSO_4 , adjusted to pH 7.3–7.4 with NaOH. The area was then covered with a coverglass. For recording of the electrocorticogram (ECoG; bandwidth 0.1–300 Hz), a thin teflon-coated silver wire (75 μm bare diameter) was slipped beneath the skull through an additional hole lateral to the craniotomy: a similar reference wire was inserted above the cerebellum. Animal temperature was maintained at 36–37°C using a heating blanket.

Intracellular recordings were obtained with sharp electrodes (resistance 70–150 M Ω) using a bridge-balance voltage amplifier (Neurodata model IR283). The electrode solution contained 0.4 M potassium acetate (buffered to pH 7.2 with HEPES), 3 or 10 mM Calcium Green-1 (CG-1; Molecular Probes, Eugene, Oregon) and, in some experiments, 2% Neurobiotin (Vector Labs, Burlingame, California). For dendritic recordings, electrodes containing 3 mM CG-1 were inserted through the agar at a shallow angle from the lateral side. For somatic recordings from layer 5 pyramidal neurons (duration, 25 min to 2 h 10 min) 10 mM CG-1 was used in the electrode to facilitate dye loading of the distal dendrites. Electrodes were inserted at a steeper angle (about 34°), and electrode tips were advanced to 800–1200 μm below the pia (corrected for surface curvature). Intrinsically bursting neurons were identified by the occurrence of spontaneous bursts and the possibility to evoke bursts by current injection.

For sensory stimulation, one to three whiskers were deflected by 5–20° in a sequence of ten square deflections at 5 Hz using a pencil lead attached to a galvanometric scanner (model 120G, General Scanning, Cambridge, Massachusetts). In some experiments, brain surface stimulation was performed using a bipolar electrode of twisted, thin, silver wires placed onto the surface in the rostral and medial corner of the craniotomy (100 μs unipolar pulses, 10–80 V).

***In vivo* calcium imaging.** *In vivo* calcium imaging was performed using a two-photon laser scanning microscope³⁵ as described³³. Briefly, a Ti:Sapphire laser (800–850 nm, 80 MHz, 100 fs pulse width; Tsunami, Spectra Physics, Mountain View, California) pumped by either a 10W Argon laser (Innova 310, Coherent, Palo Alto, California) or a 10 W diode-pumped solid-state laser (Millenia X, Spectra Physics) was used for two-photon excitation through a 40× water-immersion objective (NA 0.75, Zeiss). Galvanometric scan mirrors (6800HP, Cambridge Technology, Cambridge, Massachusetts) and data acquisition were controlled by custom software (R. Stepnoski, Lucent Technologies). Emission light was collected using a photomultiplier tube (model R3896, Hamamatsu, Bridgewater, New Jersey). To minimize photodamage, the excitation laser intensity was adjusted depending on the depth of the focal plane (lower intensity at shallower depths) and always kept at a minimum for a sufficient signal-to-noise ratio. No apparent changes in dendritic morphology, $[\text{Ca}^{2+}]$ transient kinetics or the electrical recording resulted from laser illumination. Based on the $[\text{Ca}^{2+}]$ -transient decay time constants⁵⁰ and comparison with dendritic patch recordings⁵, we estimate that the CG-1 concentration in the dendrites was $\leq 100 \mu\text{M}$, reducing and prolonging the $[\text{Ca}^{2+}]$ transients at most threefold. Since we were unable to detect dendritic Ca^{2+} influx near the main bifurcation even with multiple Na^+ APs (Figs. 1d and 3c), this does not affect our conclusion of undetectable Ca^{2+} influx with single Na^+ APs. In addition, the spatial profile of $[\text{Ca}^{2+}]$ -transient amplitude was similar in experiments using dendritic and somatic dye filling, excluding a severe distortion of the results by dye concentration gradients.

The imaging depth of 2PLSM for *in vivo* measurements currently is limited to about 500 μm ^{33,37}. Therefore, electrode tips and the lower part of the neurons could not be imaged in experiments that used impalements in layer 5. For finding and imaging dendritic tufts in these cases, electrodes were targeted to layer 5 in a region within the cranial window and devoid of large blood vessels. We filled intrinsically bursting neurons for more than 30 minutes before searching the upper layers for distal dendrites near the site expected from the depth and angle of the electrode. Typically, tuft branches were found 45–75 min following the penetration of a neuron. High-time-resolution fluorescence measurements were obtained in line-scan mode (2 ms per line) after zooming onto a dendritic location. Spatial profiles (Fig. 6) were obtained by measuring fluorescence changes at different focal depths, first along one apical tuft branch while advancing the focal plane towards the pia, and then in a different tuft branch while focusing down again. Traces obtained at the same depth were averaged. At the end of each experiment, a focus series of the entire dendritic tuft was taken ($\Delta z = 0.7$ –2 μm ; laser intensity was adjusted manually to compensate for scattering-induced fluorescence loss with depth).

Data analysis. Electrophysiological and line-scan data were analysed using IGOR software (Wavemetrics, Lake Oswego, Oregon). Amplitudes of action potentials and slow depolarizations were measured from the threshold for Na^+ APs as defined by the inflection in the voltage trace. Fluores-

cence background was measured from a region adjacent to the dendrite and subtracted. For line-scan analysis, the values of all pixels that contained dendritic fluorescence were averaged. Fluorescence traces are expressed as relative fluorescence changes $[\Delta F/F = (F - F_0)/F_0]$ where F_0 is the background-corrected pre-stimulus fluorescence. Maximum-intensity side projections of the focus series were calculated from the stack of fluorescence images using NIH Image. All data are presented as mean \pm s.e.

Histology. In some cases neurons were filled with 2% neurobiotin during the experiment. After these experiments, animals were transcardially perfused with 60 ml cold saline (0.1 M PBS) followed by 60 ml of 4% paraformaldehyde (PFA) in 0.1 M PBS. Brains were kept in 4% PFA overnight and maintained in PBS thereafter. 60 μ m-thin sections were cut on a cryomicrotome and slices were processed using the standard ABC kit (Vector Labs, Burlingame, California). Stained neurons were photographed and reconstructions were drawn by hand from several neighboring slices.

ACKNOWLEDGEMENTS

We thank G. Major and S. S.-H. Wang for comments on the manuscript and B. Burbach for help with histology. This work was supported by Lucent Technologies and the Whitehall Foundation, grants to K.S. from the NIH, the Pew and the Klingenstein Foundations and fellowships to F.H. from the Max-Planck Society and the Human Frontier Science Program.

RECEIVED 24 MAY; ACCEPTED 7 SEPTEMBER 1999

- Yuste, R. & Tank, D. W. Dendritic integration in mammalian neurons, a century after Cajal. *Neuron* 16, 701–716 (1996).
- Stuart, G., Spruston, N., Sakmann, B. & Häusser, M. Action potential initiation and backpropagation in neurons of the mammalian CNS. *Trends Neurosci.* 20, 125–131 (1997).
- Yuste, R. & Denk, W. Dendritic spines as basic functional units of neuronal integration. *Nature* 375, 682–684 (1995).
- Markram, H., Lübke, J., Frotscher, M. & Sakmann, B. Regulation of synaptic efficacy by coincidence of postsynaptic APs and EPSPs. *Science* 275, 213–215 (1997).
- Schiller, J., Schiller, Y., Stuart, G. & Sakmann, B. Calcium action potentials restricted to distal apical dendrites of rat neocortical pyramidal neurons. *J. Physiol. (Lond.)* 505, 605–616 (1997).
- Stuart, G., Schiller, J. & Sakmann, B. Action potential initiation and propagation in rat neocortical pyramidal neurons. *J. Physiol. (Lond.)* 505, 617–632 (1997).
- Caulier, L. J. & Connors, B. W. Synaptic physiology of horizontal afferents to layer I in slices of rat SI neocortex. *J. Neurosci.* 14, 751–762 (1994).
- Bernander, O., Koch, C. & Douglas, R. J. Amplification and linearization of distal synaptic input to cortical pyramidal cells. *J. Neurophysiol.* 72, 2743–2753 (1994).
- Wong, R. K. & Prince, D. A. Participation of calcium spikes during intrinsic burst firing in hippocampal neurons. *Brain Res.* 159, 385–390 (1978).
- Rhodes, P. A. & Gray, C. M. Simulations of intrinsically bursting neocortical pyramidal neurons. *Neural Comput.* 6, 1086–1110 (1994).
- Larkum, M. E., Zhu, J. J. & Sakmann, B. A new cellular mechanism for coupling inputs arriving at different cortical layers. *Nature* 398, 338–341 (1999).
- Connors, B. W. & Gutnick, M. J. Intrinsic firing patterns of diverse neocortical neurons. *Trends Neurosci.* 13, 99–104 (1990).
- Mason, A. & Larkman, A. Correlations between morphology and electrophysiology of pyramidal neurons in slices of rat visual cortex. II. Electrophysiology. *J. Neurosci.* 10, 1415–1428 (1990).
- Lisman, J. E. Bursts as a unit of neural information: making unreliable synapses reliable. *Trends Neurosci.* 20, 38–43 (1997).
- Silva, L. R., Amitai, Y. & Connors, B. W. Intrinsic oscillations of neocortex generated by layer 5 pyramidal neurons. *Science* 251, 432–435 (1991).
- Connors, B. W., Gutnick, M. J. & Prince, D. A. Electrophysiological properties of neocortical neurons in vitro. *J. Neurophysiol.* 48, 1302–1320 (1982).
- Stafstrom, C. E., Schwandt, P. C., Chubb, M. C. & Crill, W. E. Properties of persistent sodium conductance and calcium conductance of layer V neurons from cat sensorimotor cortex in vitro. *J. Neurophysiol.* 53, 153–170 (1985).
- Reuveni, I., Friedman, A., Amitai, Y. & Gutnick, M. J. Stepwise repolarization from Ca^{2+} plateaus in neocortical pyramidal cells: evidence for nonhomogeneous distribution of HVA Ca^{2+} channels in dendrites. *J. Neurosci.* 13, 4609–4621 (1993).
- Yuste, R., Gutnick, M. J., Saar, D., Delaney, K. R. & Tank, D. W. Ca^{2+} accumulations in dendrites of neocortical pyramidal neurons: an apical band and evidence for two functional compartments. *Neuron* 13, 23–43 (1994).
- Amitai, Y., Friedman, A., Connors, B. W. & Gutnick, M. J. Regenerative activity in apical dendrites of pyramidal cells in neocortex. *Cereb. Cortex* 3, 26–38 (1993).
- Kim, H. G. & Connors, B. W. Apical dendrites of the neocortex: correlation between sodium- and calcium-dependent spiking and pyramidal cell morphology. *J. Neurosci.* 13, 5301–5311 (1993).
- Seamans, J. K., Gorelova, N. A. & Yang, C. R. Contributions of voltage-gated Ca^{2+} channels in the proximal versus distal dendrites to synaptic integration in prefrontal cortical neurons. *J. Neurosci.* 17, 5936–5948 (1997).
- Schwandt, P. C. & Crill, W. E. Local and propagated dendritic action potentials evoked by glutamate iontophoresis on rat neocortical pyramidal neurons. *J. Neurophysiol.* 77, 2466–2483 (1997).
- Paré, D., Shink, E., Gaudreau, H., Destexhe, A. & Lang, E. J. Impact of spontaneous synaptic activity on the resting properties of cat neocortical pyramidal neurons in vivo. *J. Neurophysiol.* 79, 1450–1460 (1998).
- Kim, H. G., Beierlein, M. & Connors, B. W. Inhibitory control of excitable dendrites in neocortex. *J. Neurophysiol.* 74, 1810–1814 (1995).
- Paré, D., Lang, E. J. & Destexhe, A. Inhibitory control of somatodendritic interactions underlying action potentials in neocortical pyramidal neurons in vivo: an intracellular and computational study. *Neuroscience* 84, 377–402 (1998).
- McCormick, D. A., Wang, Z. & Huguenard, J. Neurotransmitter control of neocortical neuronal activity and excitability. *Cereb. Cortex* 3, 387–398 (1993).
- Pockberger, H. Electrophysiological and morphological properties of rat motor cortex neurons in vivo. *Brain Res.* 539, 181–190 (1991).
- Zhu, J. J. & Connors, B. W. Intrinsic firing patterns and whisker-evoked synaptic responses of neurons in the rat barrel cortex. *J. Neurophysiol.* 81, 1171–1183 (1999).
- Núñez, A., Amzica, F. & Steriade, M. Electrophysiology of cat association cortical cells in vivo: intrinsic properties and synaptic responses. *J. Neurophysiol.* 70, 418–430 (1993).
- Hirsch, J. A., Alonso, J. M. & Reid, R. C. Visually evoked calcium action potentials in cat striate cortex. *Nature* 378, 612–616 (1995).
- Paré, D. & Lang, E. J. Calcium electrogenesis in neocortical pyramidal neurons in vivo. *Eur. J. Neurosci.* 10, 3164–3170 (1998).
- Svoboda, K., Denk, W., Kleinfeld, D. & Tank, D. W. In vivo dendritic calcium dynamics in neocortical pyramidal neurons. *Nature* 385, 161–165 (1997).
- Svoboda, K., Helmchen, F., Denk, W. & Tank, D. W. Spread of dendritic excitation in layer 2/3 pyramidal neurons in rat barrel cortex in vivo. *Nat. Neurosci.* 2, 65–73 (1999).
- Denk, W., Strickler, J. H. & Webb, W. W. Two-photon laser scanning fluorescence microscopy. *Science* 248, 73–76 (1990).
- Denk, W. & Svoboda, K. Photon upmanship: why multiphoton imaging is more than a gimmick. *Neuron* 18, 351–357 (1997).
- Kleinfeld, D., Mitra, P. P., Helmchen, F. & Denk, W. Fluctuations and stimulus-induced changes in blood flow observed in individual capillaries in layers 2 through 4 of rat neocortex. *Proc. Natl. Acad. Sci. USA* 95, 15741–15746 (1998).
- Arieli, A., Sterkin, A., Grinvald, A. & Aertsen, A. Dynamics of ongoing activity: explanation of the large variability in evoked cortical responses. *Science* 273, 1868–1871 (1996).
- Kandel, A. & Buzsáki, G. Cellular-synaptic generation of sleep spindles, spike-and-wave discharges, and thalamocortical responses in the neocortex of rat. *J. Neurosci.* 17, 6783–6797 (1997).
- Chagnac-Amitai, Y., Luhmann, H. J. & Prince, D. A. Burst generating and regular spiking layer 5 pyramidal neurons of rat neocortex have different morphological features. *J. Comp. Neurol.* 296, 598–613 (1990).
- Tseng, G. F. & Prince, D. A. Heterogeneity of rat corticospinal neurons. *J. Comp. Neurol.* 335, 92–108 (1993).
- Baranyi, A., Szenté, M. B. & Woody, C. D. Electrophysiological characterization of different types of neurons recorded in vivo in the motor cortex of the cat. I. Patterns of firing activity and synaptic responses. *J. Neurophysiol.* 69, 1850–1864 (1993).
- Buzsáki, G. & Kandel, A. Somatodendritic backpropagation of action potentials in cortical pyramidal cells of the awake rat. *J. Neurophysiol.* 79, 1587–1591 (1998).
- Pinsky, P. F. & Rinzel, J. Intrinsic and network rhythmogenesis in a reduced Traub model for CA3 neurons. *J. Comput. Neurosci.* 1, 39–60 (1994).
- Mainen, Z. F. & Sejnowski, T. J. Influence of dendritic structure on firing pattern in model neocortical neurons. *Nature* 382, 363–366 (1996).
- Franceschetti, S. et al. Ionic mechanisms underlying burst firing in pyramidal neurons: intracellular study in rat sensorimotor cortex. *Brain Res.* 696, 127–139 (1995).
- Friedman, A. & Gutnick, M. J. Intracellular calcium and control of burst generation in neurons of guinea-pig neocortex in vitro. *Eur. J. Neurosci.* 1, 374–381 (1989).
- Wang, Z. & McCormick, D. A. Control of firing mode of corticotectal and corticopontine layer V burst-generating neurons by norepinephrine, acetylcholine, and 1S,3R-ACPD. *J. Neurosci.* 13, 2199–2216 (1993).
- Markram, H., Wang, Y. & Tsodyks, M. Differential signaling via the same axon of neocortical pyramidal neurons. *Proc. Natl. Acad. Sci. USA* 95, 5323–5328 (1998).
- Helmchen, F., Imoto, K. & Sakmann, B. Ca^{2+} buffering and action potential-evoked Ca^{2+} signaling in dendrites of pyramidal neurons. *Biophys. J.* 70, 1069–1081 (1996).